

# DEFIBRILLATION CURRENT DENSITY IMAGING

Richard S. Yoon<sup>\*</sup>, Tim P. DeMonte<sup>\*</sup>, Dawn Jorgenson<sup>†</sup>, Michael L.G. Joy<sup>\*</sup>

<sup>\*</sup> *Institute of Biomaterials and Biomedical Engineering, University of Toronto, Toronto, Canada* <sup>†</sup> *Heartstream Operation, Philips Medical Systems, Seattle, U.S.A.*

**Low frequency current density imaging (LFCDI) using a magnetic resonance (MR) imager has been shown to accurately measure electrical current density inside a phantom. CDI measures the magnetic field generated by the current and converts it to current density (CD) by computing its curl. This makes CDI an ideal technique for studying the current flow inside the body during electrical therapies such as defibrillation where the current density in tissue is closely associated with the efficacy. Here we report simultaneous measurements of current density at all points within the pig torso during an electrical current application through defibrillation electrodes. We observed current flow over the chest walls in agreement with the current literature. However, complex and unexpected current flow patterns were seen inside the heart as well as in the surrounding vasculature. This study represents the first non-invasive volume current measurement inside the pig torso during an electrical current application.**

LFCDI, [1], was performed on 4 post-mortem Yorkshire pigs weighing from 3 kg to 7 kg. Small animals were required because of the 55 cm bore of the MR imager and the three orthogonal orientations required for LFCDI. A total of 15 CDI image sets were acquired while bipolar current waveforms of 150 mA to 200 mA were applied through a set of pediatric defibrillation electrodes in equivalent position to the Anterior-Apical locations used in human defibrillation procedures. Voxel size was roughly 2 mm<sup>3</sup> with 48 cm field-of-view (256 x 256 pixels). The total time required for the experiment was 90 minutes per animal. The animal was euthanized immediately prior to imaging and lungs were kept fully inflated during the experiments.

In all four animals, the highest current density was observed in the front chest wall. As suggested by other researchers [2, 3], this high current density in the front chest area could be the result of the chest wall having lower resistance pathways between the two electrodes than the transthoracic pathway. A close examination of the CD images revealed a non-uniform current distribution within the chest wall. Higher current densities were observed in the muscles surrounding the rib cage rather than in the skin/fat layers close to the surface (Figure 1). This suggests that most of the current penetrates the skin

and travels in the underlying muscle layers. The strongest current densities were observed in the intercostal muscles near the heart and were in the range of 100 A/m<sup>2</sup> to 147 A/m<sup>2</sup> depending on the animal. Some current densities were also observed in the back and in the abdomen area as well, with an average current density of 16 A/m<sup>2</sup> and 30 A/m<sup>2</sup>, respectively (Figure 1). The total amount of current flowing over the anterior and posterior chest wall was approximately 58 % to 65 % of the applied current in all animals. Streamlines over the front chest wall are shown in Figures 2a and 2b. As expected, these streamlines were analogous to the shortest line drawn over the chest between two electrodes. Although there were some minor variations due to small differences in electrode locations, streamlines along the chest walls and in the abdomen area exhibited almost identical shapes and trajectory in all animals. These findings agree with the hypothesis that the current flow along the chest wall is closely related to the muscle fiber axis directions [2].

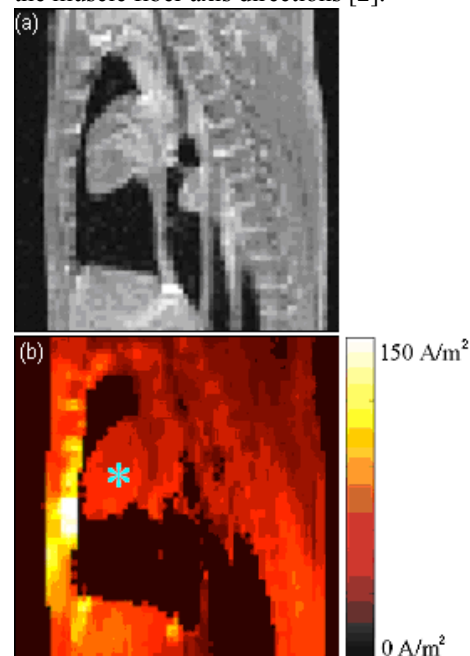


**Fig. 1** - Current density magnitude along the front chest wall. MRI magnitude image (a) and the corresponding current density image (b) illustrating the strong current density (up to 150 A/m<sup>2</sup>) along the front chest wall. This image is a sagittal slice of the pig torso with heart (marked by \*) located in the middle of the chest cavity.

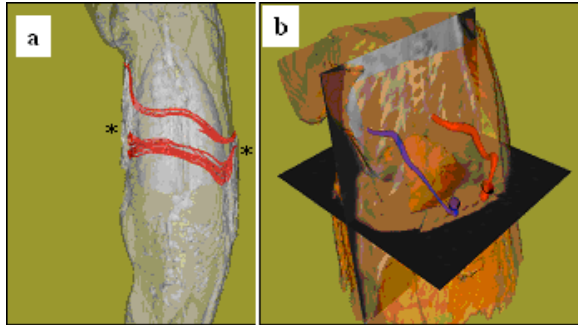


**Fig. 2** - Current flow along the chest wall. Streamlines generated from the current density data in the chest walls, seeded from the left side. Streamlines represent current pathways. Two pediatric electrodes are visible on either side of the chest (marked with \*) where the streamlines originate/terminate. a) Front view (Coronal). b) A slice of raw current density vector data from which the streamlines are drawn.

We also measured current densities inside the heart and in the surrounding vessels. The amount of current reaching the heart was approximately 18 % to 21 % of the applied current in agreement with the previous findings [2]. As expected, some of the highest current densities were observed in the myocardium closest to the chest wall (Especially in the apex of the heart where it comes in direct contact with the chest wall; maximum current density in the range of  $113 \text{ A/m}^2$  to  $189 \text{ A/m}^2$ ). Tissues further away from the chest wall generally experienced lower current density than the tissues in proximity of the chest wall. However, a detailed analysis of the heart revealed disparate current density levels in various parts of the heart. For example, average current density in the left ventricular myocardium was roughly half of that observed in the right ventricular myocardium ( $8.7 \text{ A/m}^2$  and  $22.2 \text{ A/m}^2$  respectively, Figure 3). Clear boundaries between two levels of current density in ventricles were observed along the length of the myocardial septum. Furthermore, higher current density levels were observed in blood than the surrounding myocardium ( $12.1 \text{ A/m}^2$  and  $8.8 \text{ A/m}^2$  respectively). Similar patterns of irregular current distribution were seen in all animals.

Further analysis using streamlines, revealed a complex pattern of current flow very different from those suggested by previous researchers [2]. Instead of current pathways resembling lines that connect two electrodes in a homogeneous phantom (Figure 4a), the current pathways in the ventricles were nearly orthogonal to those seen along the chest walls (Figure 4b and 4c). These seemingly contradictory directions of current flow in the ventricles and along the chest wall were consistently observed in all animals, suggesting a close relationship between the

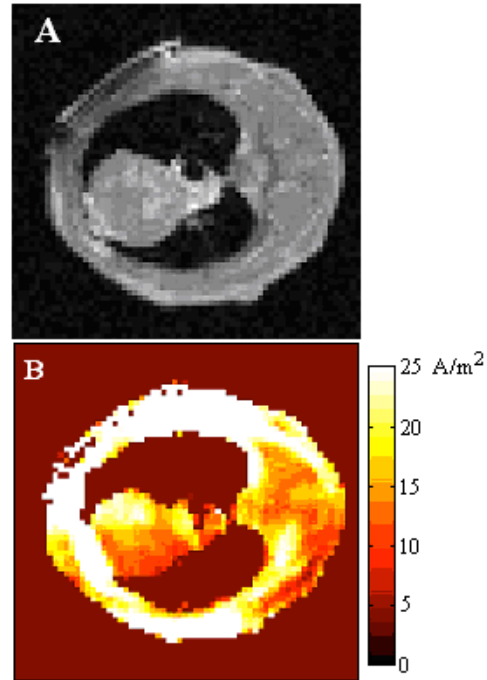


**Fig. 3** - Current density inside the heart. The upper picture (a) shows the axial MR image of the pig and the corresponding CDI image is shown below (b). Generally, a higher current density (indicated by the brighter areas) was observed over the right ventricle (yellow/white in color;  $22.2 \text{ A/m}^2$ ) than in the left ventricle (red color;  $8.7 \text{ A/m}^2$ ).

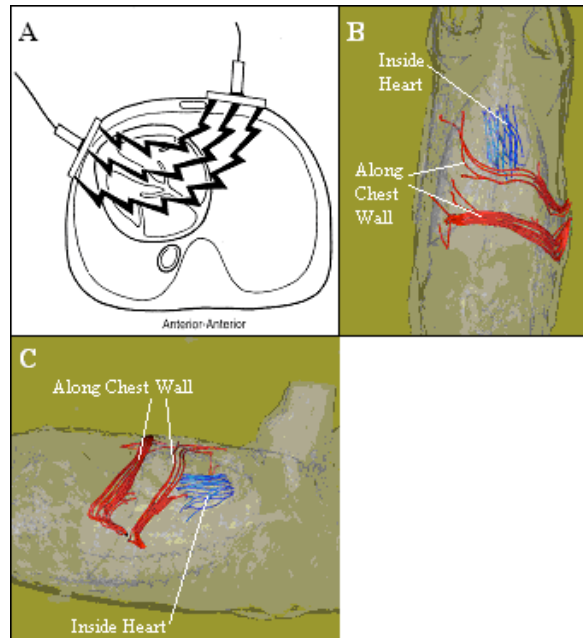


**Fig. 4** - Current pathways along the chest wall and inside the heart. Two different sets of streamlines indicate the current flow along the chest wall and inside the heart. a) A diagram indicating a traditional concept of current flow through the chest walls [1]. b) Views from the front and c) from the left side of the animal show approximately orthogonal current flow between the chest wall and the heart.

current flow and the underlying ventricular muscle fiber directions (spiral pattern towards the apex of the heart). The current entering the heart through ventricles is more likely to travel along the direction of the myocardial fiber due to the anisotropic tissue conductivity (up to 3 times higher in cardiac tissues and up to 10 times higher in skeletal muscles, [4]). The direction of current flow in the atria was different from that of the ventricles as well (Figure 5a), further reinforcing the role of the muscle fiber axis on the current flow direction (atrial myocardium is mainly organized in a ring-like manner). The boundaries between different directions of current flow were very distinct, reflecting the underlying tissue composition. For example, along the boundaries of the chest wall and the ventricle, two seemingly orthogonal current flows were separated by a distance of less than 2 mm (Figure 5b). These findings strongly suggest that inhomogeneous and anisotropic tissue conductivities play an important role in determining the current pathways in the heart.

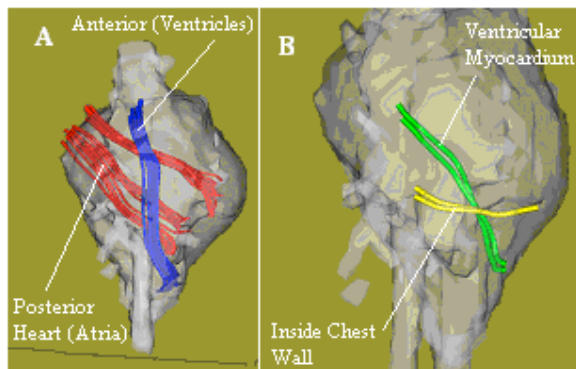


**Fig. 5** - Current streamlines inside the heart (coronal view). a) Vertical streamlines represent the current flow in the anterior portion of the ventricular myocardium close to the chest walls, while the oblique streamlines indicate the current flow in the posterior part of the heart (atria and connected vessels). b) Two groups of two streamlines near the boundary of the heart and the chest wall. Horizontal streamlines are located in the anterior chest wall and are similar to the current flow seen along the front chest wall. Vertical streamlines are located in the ventricular myocardium just 2mm below the chest wall. These seemingly contradictory current streamlines reflect the anisotropic conductivity of the underlying tissues.

In addition, we were able to identify major current entry/exit locations to/from the heart. The most prominent and the largest source of current was in the front chest wall where it comes in direct contact with the heart (Figure 6a and 6b). This region has a higher conductivity pathway to the heart than through the lung tissues that otherwise surround the heart (typical conductivities:  $\sigma_{\text{muscle}} = 0.3 \text{ S/m}$ ,  $\sigma_{\text{lung}} = 0.08 \text{ S/m}$ ; [5]). Other current pathways were observed near the right atrium and through major vessels (Vena Cava and Aorta, Figure 6c). These regions, again, provide

current pathways to the heart via tissues with conductivities higher than that of the lung. Despite variations in animal size and minor differences in electrode locations, these entry/exit points were consistent in all animals. Although CDI cannot measure current density inside the lung (limitation of the MR technique), some currents reaching the heart through lung tissues were also observed. These current flows were indicated by streamlines terminating against the heart/lung interface (Figure 6d). However, the majority of the current observed inside the heart passed through the previously mentioned pathways. The confirmation of preferential current pathways avoiding the lung (fully inflated in our experiments) reinforces recent findings, which suggest a positive correlation between the lung inspiration state and the defibrillation success rate [5].

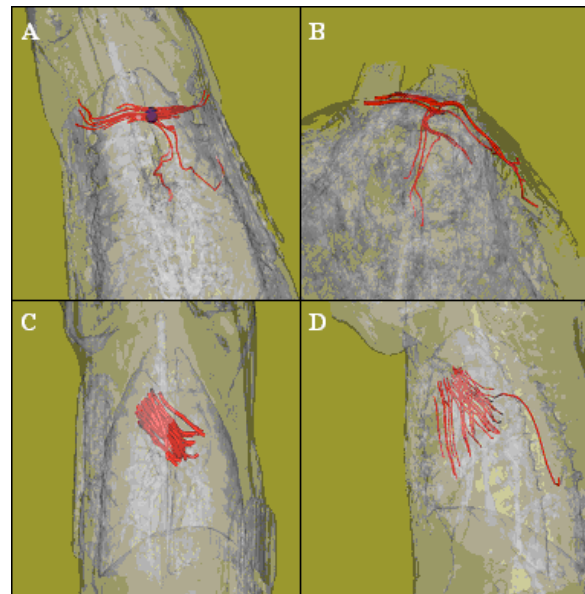


**Fig. 6** - Current streamlines indicating the entry/exit points within the heart. Majority of the current enters the heart from the front chest wall (a,b; a-axial view oblique left, b-axial view) and through right atrium (c; coronal view). Once the current enters the heart, exits via left ventricle and the connected vessels (c) to the other electrode (d; sagittal view). The streamlines shown terminating against the heart/lung interface (c,d) are a result of missing current density data from the lungs due to the low MR signal. These abrupt termination of streamlines suggest continuing current flow through the lungs.

This study, for the first time, has accurately measured the volume current density inside the post-mortem pig torso during electrical current application through defibrillation electrodes. It represents a significant step towards understanding the current pathways inside the human body during defibrillation procedures. We have shown that the current flow in the chest cavity is, to a large extent, determined by the organization and the conductivity anisotropy of

the underlying tissue. This reinforces several recent studies that have indicated the importance of anisotropic tissue conductivity in computer models of defibrillation [7, 8]. Since CDI can be easily combined with any MRI technique, measurement and comprehensive analysis of the current pathways in a live animal are feasible with the present technology, although motion and flow artifacts will create extra challenges in such experiments.

## REFERENCES

- [1] Scott, G.C., Joy, M.L.G., Armstrong, R.L. & Henkelman, R.M. Measurement of nonuniform current density by magnetic resonance. *IEEE Trans. Med. Imag.* **10**,362-374 (1991)
- [2] Tacker, W.A. Defibrillation of the heart: ICDs, AEDs, and Manual. Mosby, St. Louis 1994
- [3] Ideker, R.E., Wolf, P.D., Alferness, C., Krassowska, W. & Smith, W.M. Current concepts for selecting the location size and shape of defibrillation electrodes. *PACE* **14**,227-238 (1991)
- [4] Rush, S. Resistivity of body tissues at low frequencies. *Circ. Res.* **12**:40-XX (1963)
- [5] Stuchly, M. & Dawson, T. Interaction of Low-Frequency Electric and Magnetic Fields with the Human Body. *Proc. IEEE* **88**,643-663 (2000)
- [6] Deakin, C.D., McLaren, R.M., Petley, G.W., Clewlow, F. & Dalrymple-Hay, M.J. Effects of positive end-expiratory pressure on transthoracic impedance—implications for defibrillation. *Resuscitation* **37**,9-12 (1998)
- [7] Eason, J., Schmidt, J., Dabasinskas, A., Siekas, G., Aguel, F. & Trayanova, N. Influence of Anisotropy on Local and Global Measures of Potential Gradient in Computer models of Defibrillation. *Ann. Biomed. Eng.* **26**,840-849 (1998)
- [8] Wang, Y., Haynor, D.R. & Kim, Y. An Investigation of the Importance of Myocardial Anisotropy in Finite-Element Modeling of the Heart: Methodology and Application to the Estimation of Defibrillation Efficacy. *IEEE Trans. Biomed. Eng.* **48**,1377-1389 (2001)